Design of a Cholic Acid-based Triarmed Star Polymer Network for Targeted and Sustained Drug Delivery for Melanoma Treatment

Souvik Chowdhury[1], Swapan Maity[1], Hitesh Harsukhbhai Chandpa[2], Alok Kumar[1], Rohan Chand Sahu[2], Jairam Meena[2], Ashish Kumar Agrawal[2] and Pralay Maiti*[, 1]

[1]School of Materials Science and Technology, Indian Institute of Technology (Banaras Hindu University), Varanasi 221005, India

[2] Department of Pharmaceutical Engineering and Technology, Indian Institute of Technology (Banaras Hindu University), Varanasi 221005, India

Correspondence may be made to P. Maiti (pmaiti.mst@itbhu.ac.in)

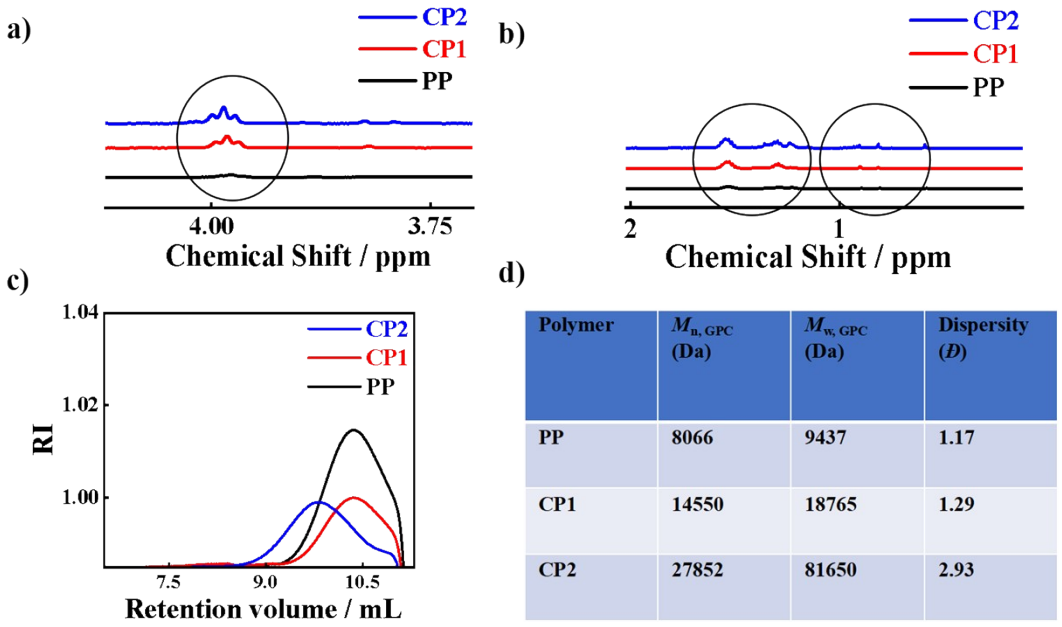

Polymer	$M_{n,GPC}$ (Da)	$M_{w,GPC}$ (Da)	Dispersity ($Đ$)
PP	8066	9437	1.17
CP1	14550	18765	1.29
CP2	27852	81650	2.93

Figure S1 :a) and b) Magnified NMR spectra of PP, CP1 and CP2. **c)** GPC chromatograms of PP, CP1, and CP2, illustrating the molecular weight distribution and shift upon chain extension and modification;**d)** Summary of molecular characteristics, including number-average molecular weight (Mn), weight-average molecular weight (Mw), and polydispersity index (Đ) for PP, CP1, and CP2, highlighting the impact of structural modification on polymer uniformity and size distribution.

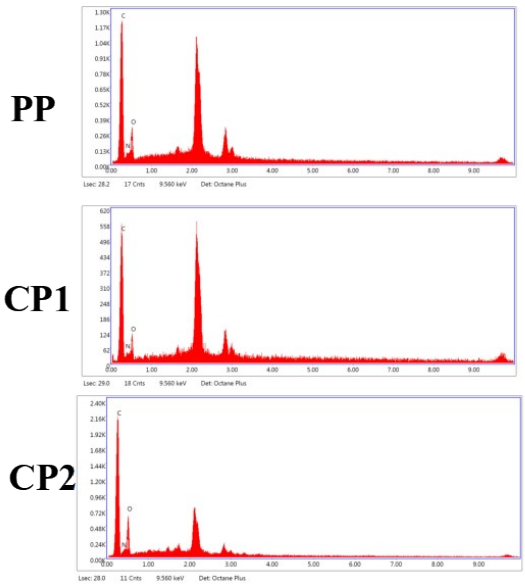

Element	Atomic %
C K	85.03
N K	0.04
O K	14.93

Element	Atomic %
C K	90.96
N K	0.11
O K	8.93

Element	Atomic %
C K	80.52
N K	1.58
O K	17.90

Figure S2: Elemental composition analysis of PP, CP1, and CP2 performed using EDAX , highlighting the presence and relative abundance of key elements, and confirming successful incorporation of functional components during polymer modification.

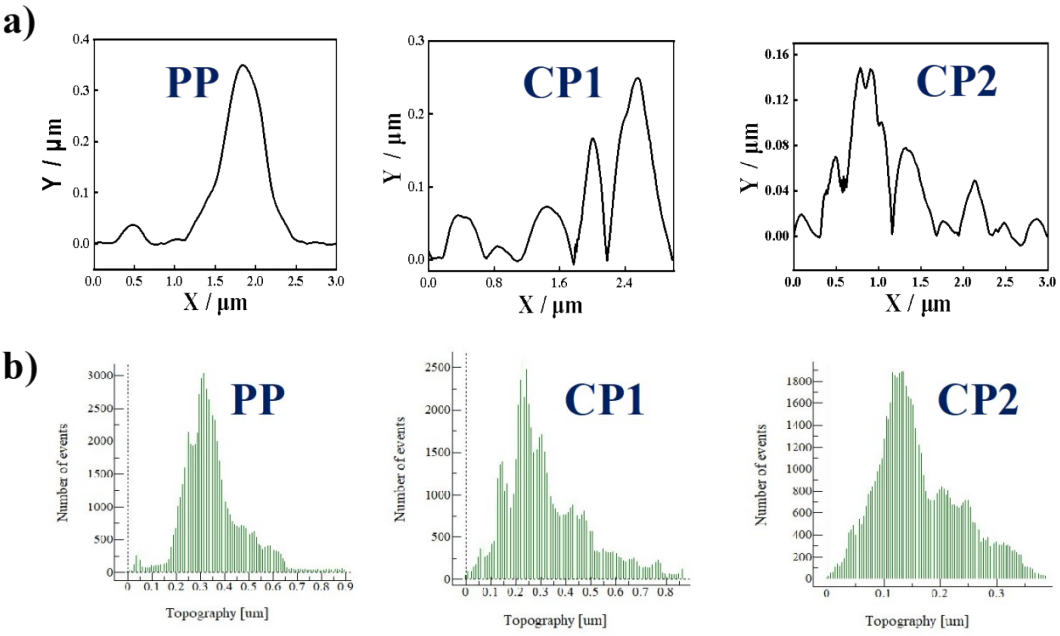

Figure S3: a) Height Profile (Cross-Sectional Roughness) of PP , CP1 and CP2. **b)** Topography Histogram (Distribution of Surface Heights) of PP, CP1 and CP2 obtained from AFM.

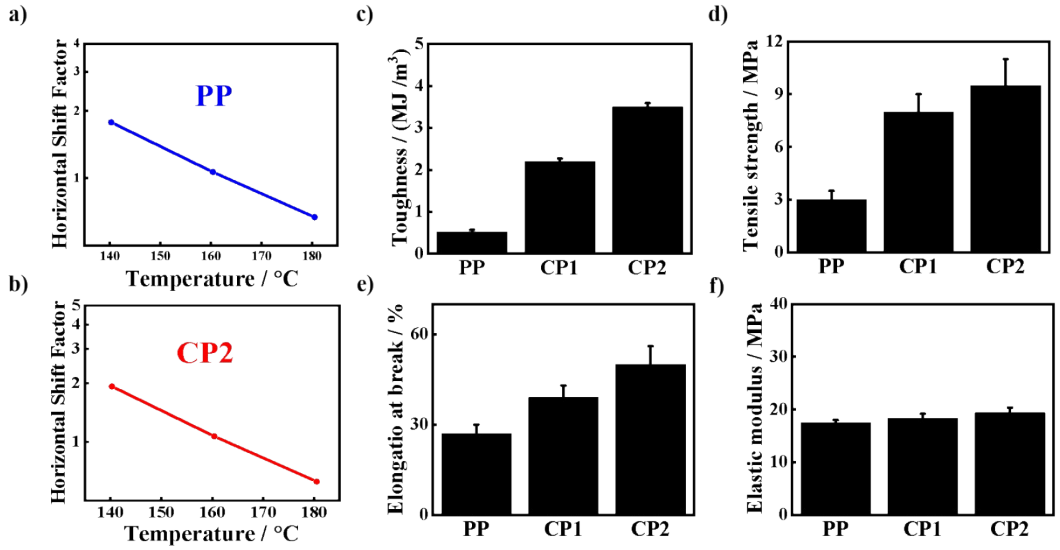

Figure S4 : Comprehensive analysis of the thermal and mechanical behavior of PP, CP1, and CP2 formulations.**a–b)** Shift factor (aT) plots for PP and CP2, demonstrating minimal deviation on either side of 160 °C, indicating thermorheological stability and consistent viscoelastic response across a temperature range;;**c-f)** Comparative mechanical analysis based on tensile stress–strain data, including:**c)** Toughness,**d)** Tensile strength, **e)** Elongation at break,, and **f)** Elastic modulus,demonstrating the influence of structural modifications on the overall mechanical performance of the materials.

a)

Sample	Zero order Model	First order Model	Krosmeyer Peppas model	Higuchi model
PP@Dox	Slope=0.56 Intercept=1.22 R^2 (COD)=0.86	Slope=0.05 Intercept=0.13 R^2 (COD)=0.89	Slope=0.34 Intercept=0.44 R^2 (COD)=0.959	Slope=1.8 Intercept=0.93 R^2 (COD)=0.966
CP1@Dox	Slope=0.30 Intercept=1.63 R^2 (COD)=0.856	Slope=0.046 Intercept=0.26 R^2 (COD)=0.853	Slope=0.24 Intercept=0.34 R^2(COD)=0.989	Slope=1.0 Intercept=1.07 R^2 (COD)=0.969
CP2@Dox	Slope=0.25 Intercept=1.93 R^2 (COD)=0.91	Slope=0.065 Intercept=0.33 R^2 (COD)=0.74	Slope=0.26 Intercept=0.22 R^2 (COD)=0.983	Slope=0.79 Intercept=0.79 R^2(COD)=0.988

b) **c)** **d)**

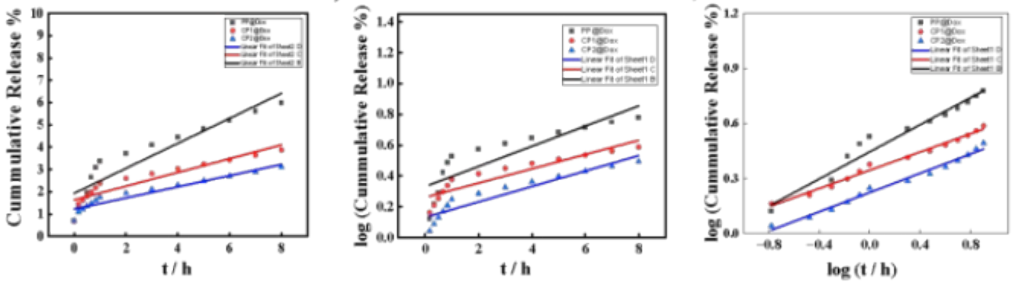

Figure S5: To elucidate the drug release behavior of the formulations, the release kinetics of Doxorubicin from PP@Dox, CP1@Dox, and CP2@Dox were systematically analyzed using various mathematical models.**a)** Summary table presenting a comparative overview of the fitting parameters and correlation coefficients for each kinetic model applied;**b)** Zero-order release model, depicting a constant drug release rate over time, independent of concentration;**c)** First-order release model, illustrating concentration-dependent release kinetics;**d)** Korsmeyer–Peppas model, providing insight into the release mechanism and diffusion behavior through the polymer matrices.

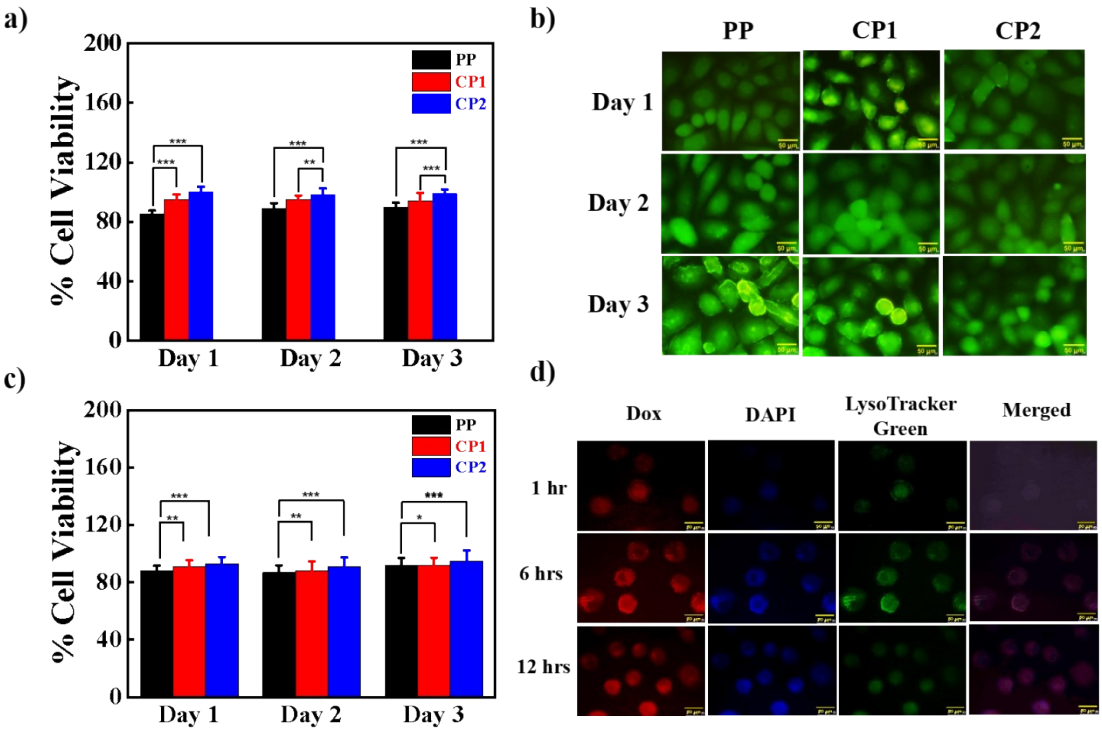

Figure S6: Evaluation of biocompatibility, in vitro cytotoxicity, and intracellular trafficking of prepolymer (PP) and cholic acid-modified polymers (CP1 and CP2), using cancerous (SiHa) and normal (3T3-L1) cell lines.**a)** MTT-based cell viability assay assessing the cytotoxic effects of PP, CP1, and CP2 (20 µg/mL) on SiHa cells. The results indicate significantly improved anti-cancer activity for the CP2 ;**b)** Fluorescence microscopy images of SiHa cells stained with acridine orange/ethidium bromide (AO/EtBr) following treatment with PP, CP1, and CP2 (all at 20 µg/mL), highlighting live and apoptotic/dead cells. Images captured at 40× magnification;**c)** In vitro biocompatibility analysis of PP, CP1, and CP2 (20 µg/mL) on 3T3-L1 fibroblast cells over different incubation periods. ;**d)** Intracellular trafficking study in cancer cells treated with CP1@Dox, tracked using LysoTracker Green (100 nM) for endo/lysosomal compartments and DAPI (5 µg/mL) for nuclear staining at various time

points. Fluorescence images acquired at 40× magnification.Data are expressed as mean ± SD (n = 3); statistical significance indicated as *p < 0.05, **p < 0.01, ***p < 0.001

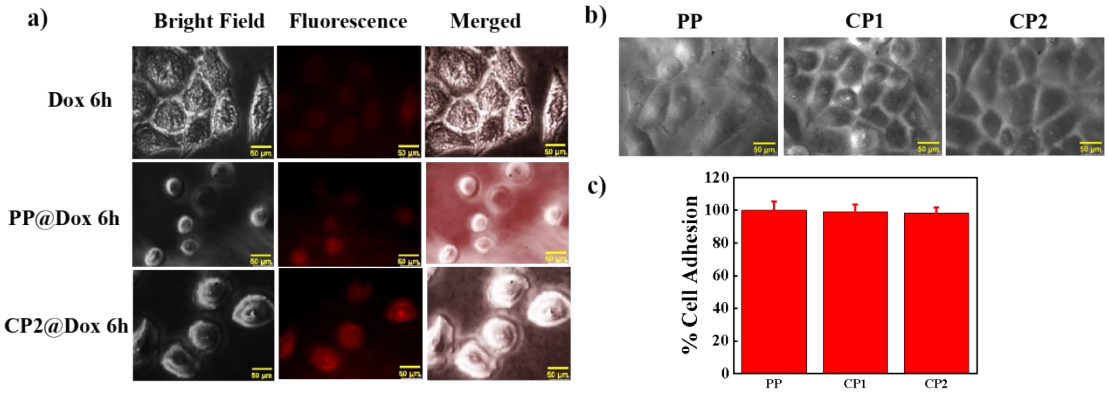

-

Figure S7: In vitro cellular evaluation of prepolymer (PP) and cholic acid-modified ppolymers (CP1 and CP2), emphasizing cellular uptake and adhesion behavior in cancer cells.**a)** Fluorescence microscopy images showing the internalization of free Dox, PP@Dox, and CP2@Dox (20 µg/mL) in cancer cells after 6 hours of incubation. Differences in fluorescence intensity reveal variation in cellular uptake efficiency among the formulations. Images captured at 40× magnification**;b)** Phase-contrast microscopy illustrating the morphology of SiHa cells cultured on surfaces treated with PP, CP1, and CP2 (20 µg/mL) after 24 hours. Distinct cellular responses indicate varying degrees of interaction with each formulation;**c)** Quantitative analysis of cell adhesion, presenting the percentage of cancer cells adhering to PP, CP1, and CP2-treated surfaces after 24 hours. CP2-treated surfaces exhibit significantly enhanced adhesion, suggesting superior cell-material affinity.Data are expressed as mean ± SD (n = 3); statistical significance indicated as *p < 0.05, **p < 0.01, ***p < 0.001

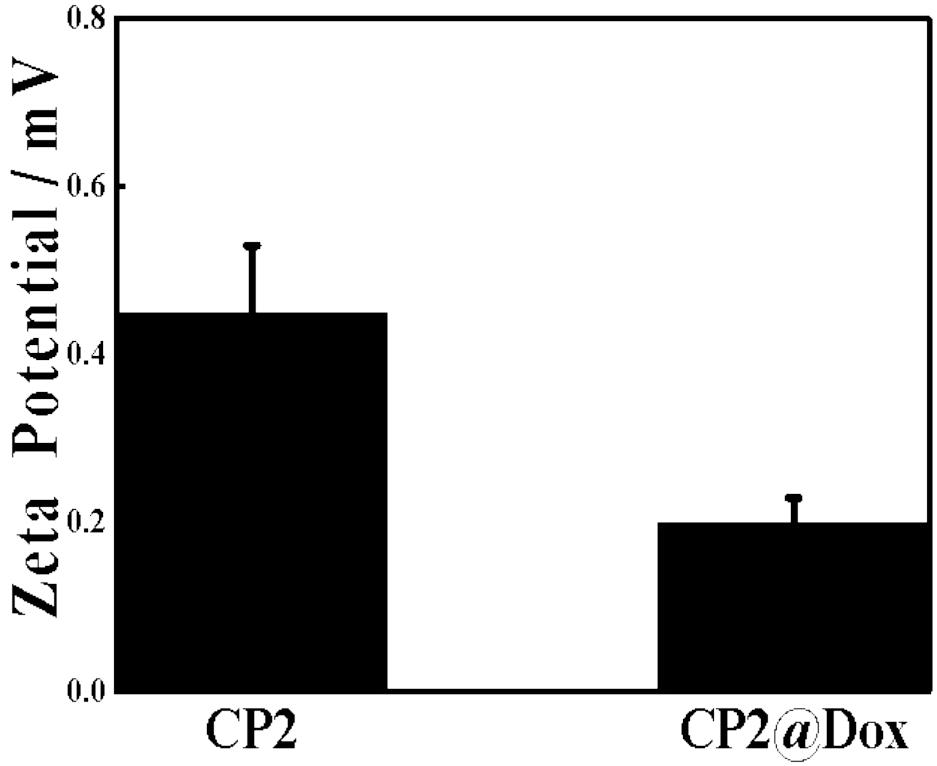

Figure S8: Zeta Potential of CP2 and CP2@Dox